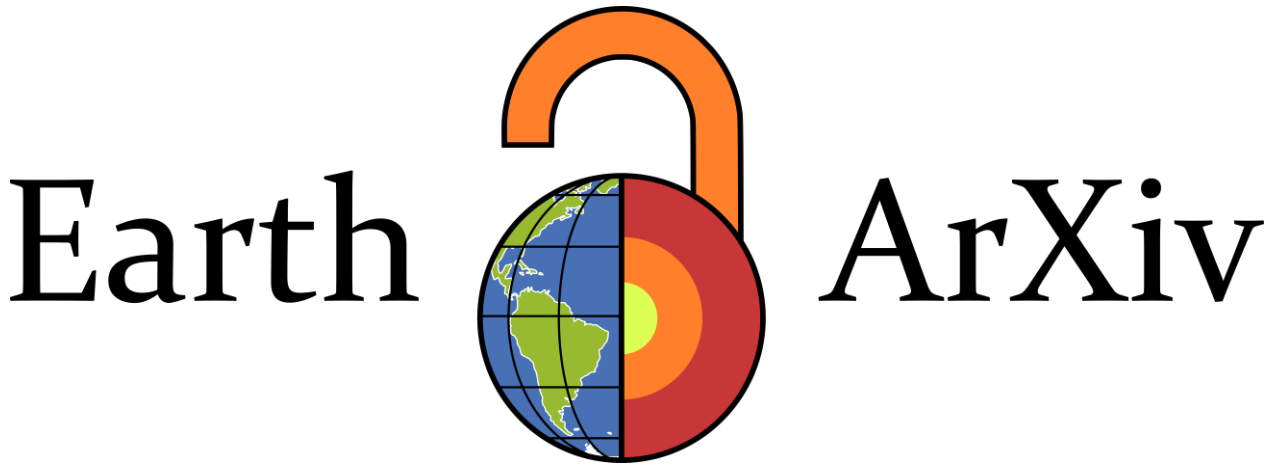

RESONANT ACTIVATION OF OXYGEN AS A HYPOTHETICAL METHOD FOR LOW-TEMPERATURE OXIDATION OF METHANE IN COAL SEAMS: THEORETICAL ANALYSIS, PARAMETRIC MODELING, AND REGIME MAPS

Olga N. Shagarova
PhD in Technical Sciences, Associate Professor
National University of Science and Technology MISIS (NUST MISIS), Moscow, Russia
Email: shagarova.on@misis.ru
ORCID: 0009-0007-8195-5827

Short Description
This paper presents a comprehensive theoretical study of a hypothetical method for low-temperature oxidation of methane directly within a coal seam. The method is based on resonant excitation of molecular oxygen by an electromagnetic field at ~1.6 MHz, corresponding to its EPR transition in the Earth's geomagnetic field. The work includes calculation of a priori determinable parameters (resonant frequencies for Kuzbass conditions, signal penetration depth), analysis of literature data on natural iron-containing catalytic centers in coals, development of a complete parametric mathematical model of the process, and construction of regime maps and nomograms. The main result is not proof of the method's feasibility (impossible without experiment), but the creation of a theoretical framework for its targeted experimental verification, including quantitative criteria for the region of practical significance and identification of critical risks such as hydrogen accumulation.

Abstract

Problem Statement. Existing methods for coal seam degassing are ineffective for methane sorbed in micropores. An alternative to extraction could be its low-temperature oxidation directly within the seam. However, known approaches require reagent injection or the creation of high temperatures. Molecular oxygen is a paramagnet and can resonantly interact with an electromagnetic field in a frequency range determined by the geomagnetic field, opening a hypothetical possibility for its selective activation without heating the medium.

Objective. To conduct a comprehensive theoretical investigation into the principal feasibility of this approach, including: (1) calculation of a priori determinable parameters (resonant frequencies, field penetration depth); (2) analysis of literature data on natural Fe-containing catalytic centers in coals; (3) development of a complete parametric mathematical model of the process; (4) construction of regime maps and nomograms covering the entire range of possible key parameter values—from demonstrably useless to potentially industrial.

Methods. Calculation of oxygen resonant frequencies within the Kuzbass geomagnetic field (IGRF-13 model). Estimation of electromagnetic signal penetration depth (skin effect theory). Literature analysis concerning EPR of oxygen, heterogeneous catalysis on iron-containing centers, and forms of iron occurrence in coals. Development of a coupled mathematical model incorporating electrodynamic, kinetic, and transport modules. Numerical parametric scanning across ranges: active site density n_{act} = 10^{12}–10^{18} m^{-2}, probability of water dissociation per period P_{diss} = 10^{-12}–10^{-2}, electrical conductivity σ = 0.001–1 S/m, emitter power P_{rad} = 1–1000 kW.

Results. Theoretical Foundations: Resonant frequencies for Kuzbass conditions are 1.59–1.64 MHz. Signal penetration depth with borehole emitter placement is 40–130 m, depending on coal resistivity. It is shown that direct electrolysis of formation water by macroscopic eddy currents is impossible. The possibility of water dissociation due to field concentration at micro-irregularities and resonant effects is a key uncertainty requiring parametric analysis. Catalytic Centers: Analysis of known Fe-containing catalytic systems (FeZSM-5, Fe-N-C materials) demonstrates the principal ability of iron to activate the C-H bond. Kuzbass coals contain ultradispersed iron particles that could potentially perform a catalytic function. The estimated active site density range is n_{act} = 10^{14}–10^{16} m^{-2}. Line Width: The EPR line width of oxygen in coal is estimated at 14–56 MHz, which relaxes stringent requirements for generator frequency stability and allows selecting a fixed frequency of 1.6 MHz for the entire Kuzbass region. Parametric Modeling: A phase diagram "site density – dissociation probability" was constructed, delineating four regions: (I) completely useless (R_{O2} < 10^{-6} kg/(m³·h)); (II) laboratory interest (10^{-6} < R_{O2} < 10^{-3}); (III) practically significant (R_{O2} > 0.75 kg/(m³·h)); (IV) industrial application (R_{O2} > 10 kg/(m³·h)). The practical significance boundary is described by the relation n_{act}·P_{diss} = 10^{9} m^{-2}. Complete performance matrices (64 combinations) and matrices for time to reach explosive hydrogen concentration (64 combinations) were generated, spanning 10 orders of magnitude in parameter variation. An analytical dependence of the effective treatment radius on coal conductivity was derived: $r_{eff} \approx 20 \cdot (0.01/\sigma)^{0.4}$ m for P_{rad} = 50 kW. For typical Kuzbass coals (σ≈0.01 S/m), the radius is ~20 m, yielding a treatment zone volume of ~25000 m³. Parameter sensitivity ranking was performed: P_{diss} and n_{act} exert the greatest influence (direct proportionality), followed by electrical conductivity σ (inverse power -1.2). Risk Analysis: It is shown that the time for diffusive removal of H_2 from the reaction zone (hours) can significantly exceed the time for accumulation of explosive concentrations (seconds to minutes) at productivities approaching industrial levels. This necessitates a forced gas extraction system for practical implementation. Energy Efficiency: A correct calculation was performed considering the entire treated volume. At a productivity of 0.75 kg O_2/(m³·h) and power of 50 kW, the specific energy consumption is ~0.01 kWh/kg CH_4. This is comparable to thermal oxidation and lower than the costs of existing degassing methods for inaccessible sorbed methane.

Conclusion. This work does not prove the viability of the proposed method—this is fundamentally impossible without experiment. However, it creates a complete theoretical framework for its targeted experimental verification. The main outcome is parametric regime maps and nomograms that allow: (a) determining under which specific conditions the method could be practical; (b) formulating quantitative requirements for system parameters; (c) identifying critical risks. The obtained results serve as a basis for designing laboratory and pilot experiments.

Keywords: *coalbed methane, degassing, electron paramagnetic resonance, geomagnetic field, formation water, low-temperature oxidation, iron catalysis, parametric modeling, regime maps, nomograms, Kuznetsk coal basin.*

INTRODUCTION

The coal industry faces two interrelated problems: the danger of methane explosions in mines and the emission of this gas as a potent greenhouse agent. According to the International Energy Agency, the coal industry accounts for about 8% of global anthropogenic methane emissions [1]. Methane has a greenhouse effect 80 times stronger than carbon dioxide over a 20-year horizon.

Traditional degassing methods, based on drilling wells, hydraulic fracturing, and creating pressure drawdown, allow extracting no more than 30–50% of the gas [2]. The main part of methane remains sorbed in coal micropores (size less than 2 nm), inaccessible to hydrodynamic stimulation. Thermal and chemical methods, such as underground gasification or in-seam combustion, require either reagent injection or the creation of high temperatures, which carries risks of spontaneous coal combustion and high energy consumption [3].

A fundamental alternative to extraction could be the neutralization of methane directly in the seam through its low-temperature oxidation. The idea considered in this work is based on three observations:

1. Molecular oxygen in its ground state ($^3\Sigma_g^-$) is a paramagnet due to its two unpaired electrons [4]. This makes it potentially sensitive to resonant exposure to an electromagnetic field in a constant magnetic field. The natural geomagnetic field of the Earth, permeating the entire lithosphere and having an induction of 55–60 μT in the Kuzbass region, could serve as this constant field.
2. Formation water is almost always present in coal seams and could, in principle, serve as a source of oxygen.
3. Coals contain iron-bearing minerals (pyrite FeS_2, siderite $FeCO_3$, as well as ultradispersed iron particles embedded in the carbon matrix [15, 16]), which could potentially perform a catalytic function.

However, between this idea and its practical implementation lie several fundamental uncertainties that cannot be resolved purely theoretically. The aim of this work is not to prove the method's viability (impossible without experiment), but to create a complete theoretical framework for it: to calculate parameters that can be determined a priori; to analyze literature data allowing an assessment of the plausibility of key assumptions; to develop a parametric mathematical model covering the entire range of unknown parameters; and to construct regime maps that will show under which specific conditions the method could be practical.

1. THEORETICAL ANALYSIS OF THE PHYSICAL FOUNDATIONS OF THE METHOD

1.1. Resonant Frequencies: Calculation Based on the Geomagnetic Field Model

This section is the only one where an unambiguous theoretical calculation, not requiring experimental verification, is possible.

The electron paramagnetic resonance (EPR) condition is described by the relation [4]:

$$h\nu = g\beta B \tag{1}$$

where h = $6.626 \cdot 10^{-34}$ J·s is Planck's constant; ν is the frequency of the alternating field, Hz; g is the spectroscopic splitting factor; β = $9.274 \cdot 10^{-24}$ J/T is the Bohr magneton; B is the induction of the constant magnetic field, T.

Molecular oxygen in its ground state is characterized by the presence of two unpaired electrons, and the g-factor remains close to 2.0 [5].

Using the IGRF-13 geomagnetic field model [6] for the territory of Kuzbass (B = 55–60 μT), we obtain a frequency range of 1.59–1.64 MHz. For the extreme values of the global geomagnetic field range (25 and 65 μT), the frequencies are 0.7 and 1.8 MHz, respectively. Thus, the sought frequencies lie in the lower part of the medium frequency (MF) band.

Table 1. EPR resonant frequencies of oxygen for Kuzbass coal seams (calculation based on the IGRF-13 model).

Geological-Economic Region	Average Induction B, μT	Resonant Frequency ν, MHz
Erunakovsky	58.2	1.63
Tersinsky	57.8	1.62
Osinovsky	58.5	1.64
Kondomsky	56.9	1.59
Mrassky	57.1	1.60

Note: Correction for local magnetic anomalies is ±15–60 kHz.

1.2. Penetration of the Electromagnetic Field into the Coal-Bearing Strata

Skin depth [7]:

$$\delta = \sqrt{\frac{2}{\omega \mu_0 \sigma}} \tag{2}$$

For ν = 1.6 MHz and the range of electrical resistivity of Kuzbass coals ρ = 10–1000 Ω·m [8], we obtain:

$$\delta \approx 500\sqrt{\rho}\ \text{m} \tag{3}$$

• For ρ = 10 Ω·m: δ ≈ 16 m
• For ρ = 100 Ω·m: δ ≈ 50 m
• For ρ = 1000 Ω·m: δ ≈ 160 m

Direct surface exposure is impossible (seam depths 300–800 m), but with the emitter placed in a borehole, the effective treatment zone (40–130 m) is sufficient for processing the near-wellbore area.

1.3. The Problem of Oxygen Generation from Formation Water

1.3.1. Macroscopic Electrolysis is Impossible

Estimate the EMF induced in a pore of radius r by an alternating magnetic field with amplitude B_0:

$$\varepsilon \approx \pi r^2 \cdot \frac{dB}{dt} = \pi r^2 \cdot 2\pi\nu B_0 \quad (4)$$

For r = 1 mm, ν = 1.6 MHz, B_0 = 1 μT:

$\varepsilon \approx 3.1 \cdot 10^{-5}$ V $= 31\ \mu$V

The decomposition potential of water, considering overpotential, is at least 1.5 V. The discrepancy by a factor of 50,000 rules out the possibility of direct electrolysis.

1.3.2. Field Concentration at Micro-irregularities

The field enhancement factor at a tip in a conducting medium [7, 10]:

$$K_{eff} = K_{vac} \cdot \frac{\omega\varepsilon\varepsilon_0}{\sigma} \quad (5)$$

For water (ε = 80), typical mineralization (σ = 0.5 S/m), and ω = 10^7 s^{-1}:

$\frac{\omega\varepsilon\varepsilon_0}{\sigma} \approx 0.014$

With K_{vac} = 10^3–10^5, we get K_{eff} = 14–1400.

If the average field in the seam E_0 ~ 1 V/m (see Section 1.5), then the local field could reach 14–1400 V/m (0.14–14 V/cm). This is insufficient for water breakdown (requires tens of kV/cm). However, other dissociation mechanisms might be possible: resonant excitation of vibrational levels, facilitated dissociation on catalytic centers, tunneling effects. None of these mechanisms can be evaluated theoretically.

Conclusion: The question of the possibility of water dissociation under these conditions remains open and is the main uncertainty, which will be accounted for later through the phenomenological parameter P_{diss} (probability of dissociation per exposure cycle).

1.4. Analysis of Possible Catalytic Mechanisms: From Known Systems to Natural Centers

1.4.1. "Inspiring Systems"

The literature describes two classes of Fe-containing systems capable of activating oxygen and oxidizing methane under mild conditions:

1. **FeZSM-5 Zeolites.** Works from the Boreskov Institute of Catalysis, SB RAS [12–14] have investigated in detail the mechanism of formation of active oxygen species (α-oxygen) on isolated iron ions in the zeolite framework. Key features: high activation temperature (400–500°C), use of N_2O as an oxygen source, reaction temperature 150–250°C. Under these conditions, α-oxygen (Fe^{3+}–O•) can selectively oxidize methane to methanol.
2. **Fe-N-C Catalysts.** Materials containing iron atoms coordinated by nitrogen within a carbon matrix exhibit high activity in the electrochemical reduction of oxygen at room temperature [17]. However, they operate in an electrocatalytic mode (with an applied potential) and in the presence of a proton-conducting membrane.

1.4.2. What Can Be Transferred to Coal?

These systems are important not as a source of kinetic parameters, but as a demonstration of the principal ability of iron, in a certain coordination environment, to activate oxygen and cleave the C-H bond of methane. They show that:

- Atomic or cluster iron can serve as an activation center.
- The process can proceed via the formation of high-valent oxo-forms (Fe^{4+}=O) or peroxo complexes.
- High temperature is not always required for activation—in electrochemical systems, it is successfully replaced by potential.

The fundamental difference between the proposed approach and known catalytic systems lies in the method of activation. In FeZSM-5, activation requires high temperature (400–500°C) and the use of N_2O as an oxidant [12–14]. In Fe-N-C materials, catalysis occurs in an electrochemical cell with controlled potential [17]. In our case, the activating factor is the alternating electromagnetic field at 1.6 MHz, which could create local micro-potentials on the surface of Fe-centers. This regime is poorly studied, and the possibility of a direct analogy with known systems requires experimental verification.

Kuzbass coals contain ultradispersed iron particles embedded in the carbon matrix [15, 16]. According to Mössbauer spectroscopy data, their coordination environment differs from pyrite and bulk oxides. Theoretically, it cannot be ruled out that under the influence of an alternating field, these centers might exhibit activity analogous to Fe-N-C materials.

However, direct transfer is impossible due to:

- Unknown structure of the centers in coal.
- Absence of a controlled potential (instead, an alternating field).
- Low temperature (30–50°C).
- Presence of water, which could block the centers.

1.4.3. Estimation of Active Site Density in Kuzbass Coals

Based on literature data [15, 16] for Kuzbass coals:

- Total Fe content: 0.5–3% (mass)
- Fraction of ultradispersed (potentially active) fraction: 10–30%
- Specific pore surface area: $S_{sp} = 10^4$ m²/m³ [11]

The estimated active site density yields a range:

$$n_{act} = 10^{14}–10^{16}\ \text{m}^{-2}$$

This range will be used in parametric modeling.

1.5. Line Width and Equipment Requirements

Estimation of the EPR line width of oxygen adsorbed on a carbon surface, according to data [20], gives ΔB = 0.5–2.0 mT, which in frequency terms corresponds to 14–56 MHz. This means that requirements for generator frequency stability are minimal (tolerance ~160 kHz). Inhomogeneous broadening due to geomagnetic field variations contributes ±140 kHz, which is also not problematic with a line width of 14–56 MHz.

Conclusion: A frequency of 1.6 MHz could be selected once and for all for the entire Kuzbass region.

1.6. Preliminary Estimation of Emitter Power and Field Strength

To estimate the required power, consider a vertical magnetic dipole placed in a borehole. In the near zone, the amplitude of the magnetic field at a distance r from a dipole with moment M can be estimated as [9]:

$$B \approx \frac{\mu_0 M}{2\pi r^3} e^{-r/\delta} \qquad (6)$$

The magnetic moment of the dipole is related to the current I in the coil, number of turns N, and area S: M = I N S.

For typical parameters: r = 10 m, δ = 50 m, required B_0 = 1 μT. From (6), the required magnetic moment is:

$$M \approx \frac{2\pi B_0 r^3}{\mu_0} e^{r/\delta} \approx \frac{2\pi \cdot 10^{-6} \cdot 1000}{4\pi \cdot 10^{-7}} \cdot e^{0.2} \approx 5000 \cdot 1.22 \approx 6100\ \text{A}\cdot\text{m}^2$$

For a coil with radius 0.5 m (area ~0.78 m²), this requires I N ≈ 7800 A·turns. At a current of 100 A, 78 turns are needed. The power dissipated in such a coil would be on the order of 50–100 kW. This estimate will be refined in parametric modeling.

2. COMPLETE MATHEMATICAL MODEL OF THE PROCESS

2.1. Model Structure

A coupled mathematical model was developed, consisting of three modules:

1. **Electrodynamic module** — distribution of the magnetic field from a borehole emitter in the coal-bearing strata.
2. **Kinetic module** — surface reactions on Fe-containing centers leading to the generation of oxygen and hydrogen.
3. **Transport module** — diffusion of gases (especially H_2) in the porous medium and the explosion safety criterion.

2.2. Electrodynamic Module

Distribution of the magnetic field from a vertical magnetic dipole placed in a borehole, in cylindrical coordinates (r, z):

$$B(r,z) = \frac{\mu_0 M}{4\pi} \cdot \frac{1}{(r^2+z^2)^{3/2}} \cdot e^{-r/\delta(\sigma)} \cdot f(z) \quad (7)$$

where M = I N S is the magnetic moment, δ(σ) is the skin depth (2), and f(z) is a function accounting for the finite length of the emitter (for simplicity in further analysis, we consider the cross-section z=0 where the field is maximum).

The electric field induced in the medium:

$$E(r) \approx \frac{\omega B(r) r}{2} \quad (8)$$

This value is used to estimate field concentration at micro-irregularities (Section 1.3.2).

2.3. Kinetic Module

2.3.1. Main Assumptions

1. Active centers are iron atoms/clusters on the pore surface with density n_{act} [m^{-2}].
2. Water molecules adsorb onto these centers.
3. Under the influence of the alternating magnetic field, with probability P_{diss} per oscillation period, dissociation of an adsorbed water molecule occurs. Thus, P_{diss} is a dimensionless probability of dissociation per period.
4. Dissociation products (OH radicals, atomic oxygen) react with methane, also adsorbed on the surface or in the immediate vicinity.
5. Final products are CO_2 and H_2O (complete oxidation) or CO, H_2 (incomplete oxidation). To estimate oxygen productivity and the risk of hydrogen accumulation, considering the stoichiometry of water decomposition is sufficient.

2.3.2. System of Kinetic Equations

Let us introduce the following variables:

- θ_{H2O} — fraction of centers occupied by adsorbed water
- θ_O — fraction of centers where active oxygen has formed
- $\theta_{tot} = \theta_{H2O} + \theta_O$ — total fraction of occupied centers

System of equations:

$$\frac{d\theta_{H_2O}}{dt} = k_{ads} P_{H_2O} (1 - \theta_{tot}) - k_{des} \theta_{H_2O} - k_{diss}(B,\nu)\theta_{H_2O} \quad (9)$$

$$\frac{d\theta_O}{dt} = 2k_{diss}(B,\nu)\theta_{H_2O} - k_{reac}\theta_O \theta_{CH_4} \quad (10)$$

where:

- k_{ads} — adsorption rate constant for water

- k_{des} — desorption rate constant for water
- k_{reac} — reaction rate constant for active oxygen with methane
- P_{H2O} — partial pressure of water vapor (under reservoir conditions, close to the saturated vapor pressure at given temperature)
- θ_{CH4} — fraction of centers occupied by methane (for productivity estimation, we assume $\theta_{CH4} \approx 1$, as methane is the main component of the gas phase in the seam)

The key element of the model is the dissociation rate constant $k_{diss}(B,\nu)$, which links the field frequency and the probability of dissociation per period:

$$k_{diss}(B, \nu) = \nu \cdot P_{diss} \cdot \left(\frac{B}{B_0}\right)^2 \cdot g(\nu - \nu_0) \quad (11)$$

where:

- P_{diss} — dimensionless probability of dissociation of a water molecule adsorbed on an active center, per one period of the electromagnetic field oscillation at frequency ν.
- The factor ν converts the probability per period into an event frequency per second.
- $B_0 = 1$ μT — reference field value
- $g(\Delta\nu)$ — line shape function (Lorentzian with width $\Delta\nu_{1/2} = 30$ MHz, based on estimates in Section 1.5)

It should be noted that in the proposed model, the frequency ν serves two functions. First, it determines the condition for resonant interaction with molecular oxygen (via the line shape function $g(\Delta\nu)$ in equation (11)). Second, it sets the rate of water dissociation (the factor ν). In this first approximation, the dissociation probability per period P_{diss} itself is considered independent of frequency within the oxygen EPR line width. This simplification is based on the assumption that resonant excitation of oxygen facilitates water dissociation, but the detailed mechanism of this coupling requires separate investigation.

2.3.3. Steady-State Solution and Productivity

In the steady state ($d\theta/dt = 0$), from (9)-(10) we obtain:

$$\theta_{H_2O} = \frac{k_{ads} P_{H_2O}}{k_{ads} P_{H_2O} + k_{des} + k_{diss}} \quad (12)$$

Under reservoir conditions, water adsorption is strong (high P_{H2O}), so we can assume $\theta_{H2O} \approx 1$ (all centers occupied by water). Then the rate of active oxygen generation is:

$$R_O = 2 k_{diss} \cdot n_{act} \cdot S_{sp} \quad (13)$$

The rate of molecular oxygen generation (assuming two active O atoms recombine into O_2 or participate in two oxidation acts) is:

$$R_{O_2} = \frac{1}{2} R_O = k_{diss} \cdot n_{act} \cdot S_{sp} \quad (14)$$

Substituting (11) into (14), with $\theta_{H2O} \approx 1$, $B = B_0$, $\Delta\nu = 0$ (exact resonance), we obtain the main relation for productivity:

$$R_{O_2} = S_{sp} \cdot n_{act} \cdot \nu \cdot P_{diss} \quad (15)$$

Dimensions: $[S_{sp}] = m^2/m^3$, $[n_{act}] = m^{-2}$, $[\nu] = s^{-1}$, P_{diss} is dimensionless. Consequently, R_{O2} has dimension $[s^{-1} \cdot m^{-3}]$, which, after multiplying by the mass of an O_2 molecule, yields $kg/(m^3 \cdot s)$. For conversion to $kg/(m^3 \cdot h)$, the factor 3600 is used.

The rate of hydrogen generation (from stoichiometry $2H_2O \rightarrow 2H_2 + O_2$) is:

$$R_{H_2} = 2 R_{O_2} \cdot \frac{M_{H_2}}{M_{O_2}} = 2 R_{O_2} \cdot \frac{2}{32} = 0.125 R_{O_2} \text{ (in mass units)} \quad (16)$$

Red: < 0.001 (useless) | Yellow: 0.001–0.1 (lab interest) | Green: 0.1–10 (practically significant) | Blue: > 10 (industrial)

Table 2. Estimated productivity R_{O2} [kg/(m³·h)] for various combinations of n_{act} and P_{diss}

P_{diss} ↓ / n_{act} →	10^{12}	10^{13}	10^{14}	10^{15}	10^{16}	10^{17}	10^{18}
10^{-12}	**$5.8\cdot10^{-11}$** (<0.001)	**$5.8\cdot10^{-10}$** (<0.001)	**$5.8\cdot10^{-9}$** (<0.001)	**$5.8\cdot10^{-8}$** (<0.001)	**$5.8\cdot10^{-7}$** (<0.001)	**$5.8\cdot10^{-6}$** (<0.001)	**$5.8\cdot10^{-5}$** (<0.001)
10^{-11}	**$5.8\cdot10^{-10}$** (<0.001)	**$5.8\cdot10^{-9}$** (<0.001)	**$5.8\cdot10^{-8}$** (<0.001)	**$5.8\cdot10^{-7}$** (<0.001)	**$5.8\cdot10^{-6}$** (<0.001)	**$5.8\cdot10^{-5}$** (<0.001)	**$5.8\cdot10^{-4}$** (<0.001)
10^{-10}	**$5.8\cdot10^{-9}$** (<0.001)	**$5.8\cdot10^{-8}$** (<0.001)	**$5.8\cdot10^{-7}$** (<0.001)	**$5.8\cdot10^{-6}$** (<0.001)	**$5.8\cdot10^{-5}$** (<0.001)	$5.8\cdot10^{-4}$ (0.001-0.1)	0.0058 (0.001-0.1)
10^{-9}	**$5.8\cdot10^{-8}$** (<0.001)	**$5.8\cdot10^{-7}$** (<0.001)	**$5.8\cdot10^{-6}$** (<0.001)	**$5.8\cdot10^{-5}$** (<0.001)	$5.8\cdot10^{-4}$ (0.001-0.1)	0.0058 (0.001-0.1)	0.058 (0.001-0.1)
10^{-8}	**$5.8\cdot10^{-7}$** (<0.001)	**$5.8\cdot10^{-6}$** (<0.001)	**$5.8\cdot10^{-5}$** (<0.001)	$5.8\cdot10^{-4}$ (0.001-0.1)	0.0058 (0.001-0.1)	0.058 (0.001-0.1)	**0.58** (0.1-10)
10^{-7}	**$5.8\cdot10^{-6}$** (<0.001)	**$5.8\cdot10^{-5}$** (<0.001)	$5.8\cdot10^{-4}$ (0.001-0.1)	0.0058 (0.001-0.1)	0.058 (0.001-0.1)	**0.58** (0.1-10)	**5.8** (0.1-10)
10^{-6}	**$5.8\cdot10^{-5}$** (<0.001)	$5.8\cdot10^{-4}$ (0.001-0.1)	0.0058 (0.001-0.1)	0.058 (0.001-0.1)	**0.58** (0.1-10)	**5.8** (0.1-10)	**58** (>10)
10^{-5}	$5.8\cdot10^{-4}$ (0.001-0.1)	0.0058 (0.001-0.1)	0.058 (0.001-0.1)	**0.58** (0.1-10)	**5.8** (0.1-10)	**58** (>10)	**580** (>10)
10^{-4}	0.0058 (0.001-0.1)	0.058 (0.001-0.1)	**0.58** (0.1-10)	**5.8** (0.1-10)	**58** (>10)	**580** (>10)	5800
10^{-3}	0.058 (0.001-0.1)	**0.58** (0.1-10)	**5.8** (0.1-10)	**58** (>10)	**580** (>10)	5800	58000

2.4. Transport Module and Hydrogen Safety Analysis

Diffusion equation for hydrogen in a porous medium with source term:

$$\frac{\partial C_{H_2}}{\partial t} = D_{eff}\nabla^2 C_{H_2} + R_{H_2}(r) \tag{18}$$

where C_{H2} is hydrogen concentration [kg/m³], D_{eff} is the effective diffusion coefficient in the porous medium:

$$D_{eff} = \frac{D_0 \cdot \phi}{\tau} \cdot \frac{1}{1+K_H} \tag{19}$$

- D_0 — diffusion coefficient of H_2 in methane (under reservoir conditions ~0.1 cm²/s = 10^{-5} m²/s)
- φ — porosity (0.02–0.15)
- τ — tortuosity (typical value 2–5)
- K_H — Henry's constant for H_2 sorption by coal (negligible for hydrogen [33])

Characteristic diffusion time over distance L:

$$t_{diff} \approx \frac{L^2}{D_{eff}} \tag{20}$$

Explosion safety criterion (lower explosive limit for H_2 in air mixture — 4%):

$$C_{H_2}(r,z,t) < 0.04 \cdot C_{gas} \tag{21}$$

where C_{gas} is the total gas phase concentration in pores ($\sim \rho_{gas} \cdot \varphi$).

Let us estimate the time to reach explosive concentration in a closed volume (ignoring diffusion). Gas volume in 1 m³ of coal: $V_{gas} = \varphi$. Mass of H_2 to reach 4%:

$$M_{H_2}^{4\%} = 0.04 \cdot \rho_{H_2} \cdot \phi \tag{22}$$

For $\varphi = 0.05$, $\rho_{H2} = 0.09$ kg/m³ (reservoir conditions): $M_{H2}{}^{4\%} = 1.8 \cdot 10^{-4}$ kg/m³.

Accumulation time:

$$t_{4\%} = \frac{M_{H_2}^{4\%}}{R_{H_2}} \tag{23}$$

Green: > 3600 s (> 1 hour) — safe | Yellow: 60–3600 s (1 min – 1 hour) — requires control | Red: < 60 s — explosive

Table 3. Time to reach explosive H_2 concentration [seconds] in a closed volume ($\varphi = 0.05$, no diffusion)

P_{diss} ↓ / n_{act} →	10^{12}	10^{13}	10^{14}	10^{15}	10^{16}	10^{17}	10^{18}
10^{-12}	$3.4 \cdot 10^{7}$ (>3600 s)	$3.4 \cdot 10^{6}$ (>3600 s)	$3.4 \cdot 10^{5}$ (>3600 s)	$3.4 \cdot 10^{4}$ (>3600 s)	3400 (60-3600 s)	340 (60-3600 s)	34 (<60 s)
10^{-11}	$3.4 \cdot 10^{6}$ (>3600 s)	$3.4 \cdot 10^{5}$ (>3600 s)	$3.4 \cdot 10^{4}$ (>3600 s)	3400 (60-3600 s)	340 (60-3600 s)	34 (<60 s)	3.4 (<60 s)
10^{-10}	$3.4 \cdot 10^{5}$ (>3600 s)	$3.4 \cdot 10^{4}$ (>3600 s)	3400 (60-3600 s)	340 (60-3600 s)	34 (<60 s)	3.4 (<60 s)	0.34 (<60 s)
10^{-9}	$3.4 \cdot 10^{4}$ (>3600 s)	3400 (60-3600 s)	340 (60-3600 s)	34 (<60 s)	3.4 (<60 s)	0.34 (<60 s)	0.034 (<60 s)
10^{-8}	3400 (60-3600 s)	340 (60-3600 s)	34 (<60 s)	3.4 (<60 s)	0.34 (<60 s)	0.034 (<60 s)	0.0034 (<60 s)
10^{-7}	340 (60-3600 s)	34 (<60 s)	3.4 (<60 s)	0.34 (<60 s)	0.034 (<60 s)	0.0034 (<60 s)	$3.4 \cdot 10^{-4}$ (<60 s)
10^{-6}	34 (<60 s)	3.4 (<60 s)	0.34 (<60 s)	0.034 (<60 s)	0.0034 (<60 s)	$3.4 \cdot 10^{-4}$ (<60 s)	$3.4 \cdot 10^{-5}$ (<60 s)
10^{-5}	3.4 (<60 s)	0.34 (<60 s)	0.034 (<60 s)	0.0034 (<60 s)	$3.4 \cdot 10^{-4}$ (<60 s)	$3.4 \cdot 10^{-5}$ (<60 s)	$3.4 \cdot 10^{-6}$ (<60 s)
10^{-4}	0.34 (<60 s)	0.034 (<60 s)	0.0034 (<60 s)	$3.4 \cdot 10^{-4}$ (<60 s)	$3.4 \cdot 10^{-5}$ (<60 s)	$3.4 \cdot 10^{-6}$ (<60 s)	$3.4 \cdot 10^{-7}$ (<60 s)
10^{-3}	0.034 (<60 s)	0.0034 (<60 s)	$3.4 \cdot 10^{-4}$ (<60 s)	$3.4 \cdot 10^{-5}$ (<60 s)	$3.4 \cdot 10^{-6}$ (<60 s)	$3.4 \cdot 10^{-7}$ (<60 s)	$3.4 \cdot 10^{-8}$ (<60 s)

Characteristic diffusion removal time over distance L = 1 m (typical block size between fractures) with $D_{eff} \sim 10^{-6}$ m²/s (considering porosity and tortuosity):

$$t_{diff} \approx \frac{1^2}{10^{-6}} = 10^6 \text{ s} \approx 11.6 \text{ days}$$

For L = 0.1 m (closer to a drainage fracture): $t_{diff} \approx 10^4$ s ≈ 2.8 hours.

Comparison of Table 3 with these estimates shows that in the region of practical significance (green cells in Table 2), hydrogen accumulation time is seconds to minutes, orders of magnitude less than diffusion removal time. Consequently, for productivity > 0.1 kg/(m³·h), a forced gas extraction system is necessary.

2.5. Practical Significance Threshold

To estimate the threshold productivity, consider a typical pilot project scenario:

- Treated volume: near-wellbore zone radius 20 m, seam thickness 5 m → V ≈ 6280 m³
- Methane content in this volume: with average methane content 20 m³/t, coal density 1.4 t/m³ → $M_{CH4} \approx 20 \cdot 1.4 \cdot 6280 \approx 175{,}840$ m³ ≈ 126,000 kg

- Oxidizing 1 kg of CH_4 requires 4 kg of O_2 (stoichiometry $CH_4 + 2O_2 \rightarrow CO_2 + 2H_2O$). Required O_2 mass: ~504,000 kg.
- Acceptable treatment time: ~100 hours (4 days)

Required oxygen productivity:

$$R_{O_2}^{req} = \frac{504000}{6280 \cdot 100} \approx 0.8 \text{ kg}/(\text{m}^3 \cdot \text{h})$$

We adopt a threshold value of 0.75 kg/(m³·h). From Table 2 we obtain the threshold condition:

$$n_{act} \cdot P_{diss} > 10^9 \text{ m}^{-2} \quad (24)$$

Figure 1. Phase diagram "Site density – Dissociation probability"

Zone I: useless (R<0.001) | Zone II: lab interest (0.001-0.1) | Zone III: practically significant (0.1-10)

Zone IV: industrial (>10) | Red line – threshold 0.75 kg/(m³·h) | Blue dash – t₄% = 1 hour

Fig. 1. Phase diagram

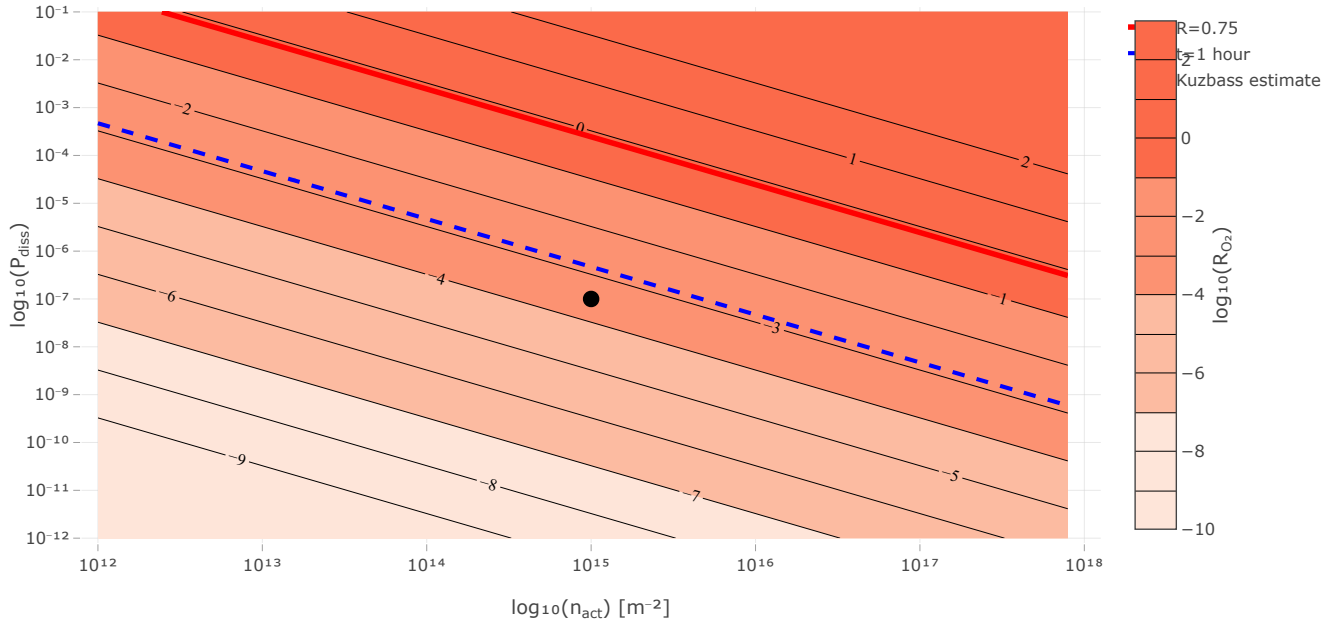

3. PARAMETRIC MODELING: METHODOLOGY AND RESULTS

3.1. Parameter Ranges for Modeling

Table 4. Ranges of varied parameters

Parameter	Symbol	Minimum	Maximum	Dimension
Coal conductivity	σ	0.001	1.0	S/m
Porosity	φ	0.02	0.15	rel. units
Density of Fe centers	n_{act}	10^{12}	10^{18}	m^{-2}
Dissociation probability	P_{diss}	10^{-12}	10^{-2}	rel. units
Emitter power	P_{rad}	1	1000	kW
Frequency	ν	1.5	1.7	MHz

3.3. Influence of Coal Electrical Conductivity

Table 5. Effective treatment zone [radius in meters] for B > 0.5 μT, P_{rad} = 50 kW

σ [S/m]	ρ [Ω·m]	δ [m]	r_{eff} [m]	Volume V_{eff} [m^3]
0.001	1000	160	42	83200
0.002	500	113	35	57700
0.005	200	71	26	35400
0.01	100	50	20	25100
0.02	50	35	15	14100
0.05	20	22	10	7850
0.1	10	16	7	3850
0.2	5	11	5	1960
0.5	2	7	3	850
1.0	1	5	2	420

Approximation:

$$r_{eff} \approx 20 \cdot \left(\frac{0.01}{\sigma}\right)^{0.4} \text{m} \quad (25)$$

Figure 2. Nomogram for engineering calculation (P_{rad} = 50 kW)

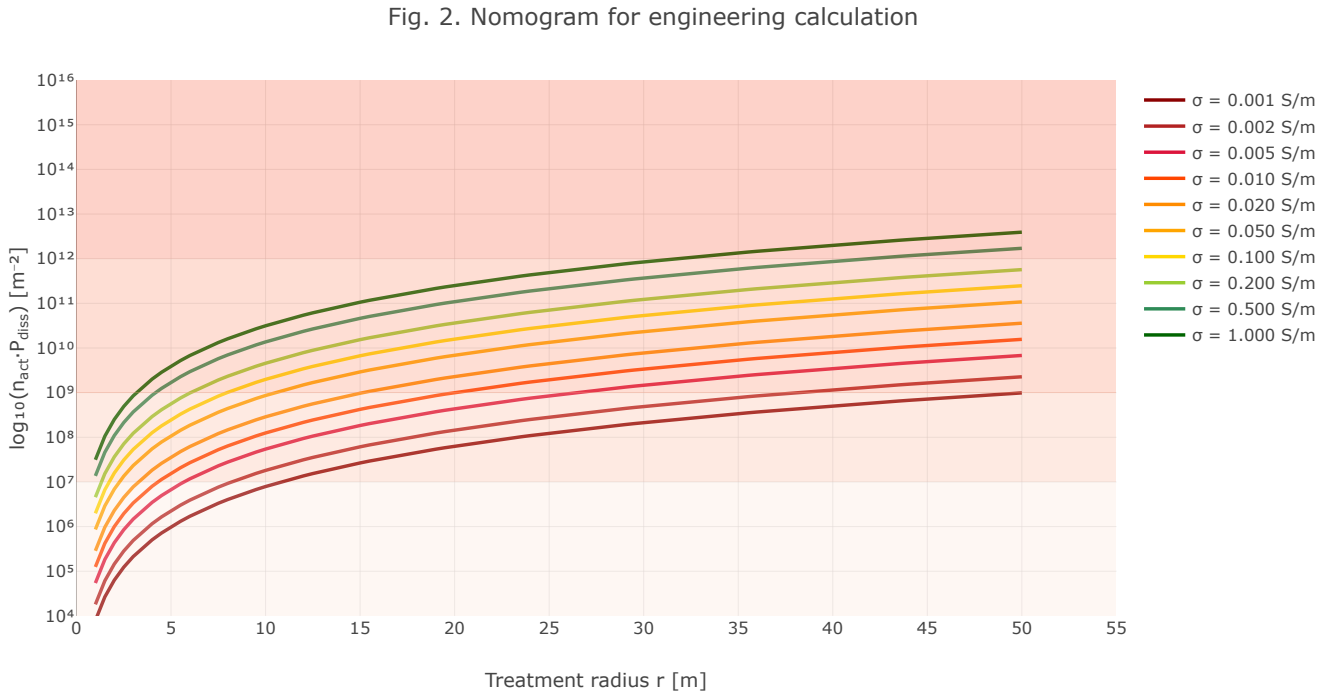

3. Calculate $P_{diss} = (n \cdot P)_{req} / n_{act}$
4. If $P_{diss} > 10^{-7}$ — the method is promising

Figure 3. Dependence of effective treatment radius on coal conductivity

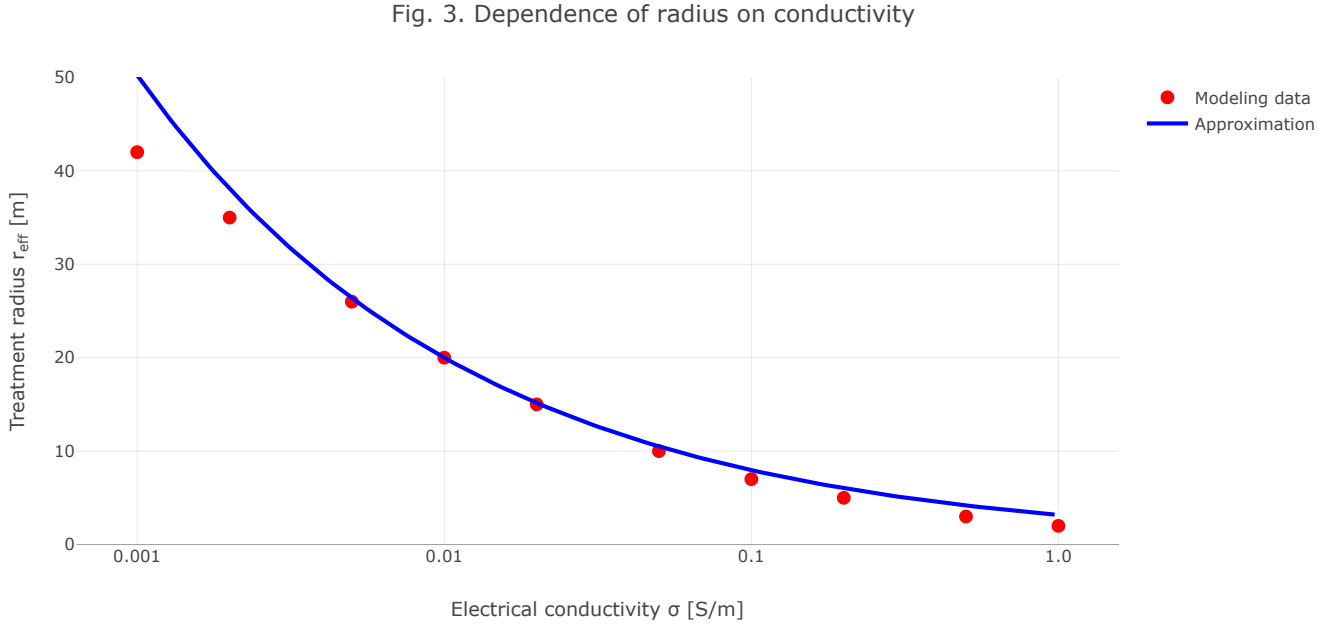

3.4. Energy Tables

Table 6. Required emitter power [kW] to achieve B = 1 μT at radius r (axisymmetric problem, central cross-section)

r [m] → σ [S/m] ↓	5	10	15	20	25	30	40	50
0.001	0.8	3	7	13	22	35	75	145
0.005	1.2	6	16	35	65	115	290	620
0.01	1.5	9	27	62	125	235	650	1480
0.05	3	28	115	340	840	1850	—	—
0.1	4	52	260	920	—	—	—	—
0.5	7	210	—	—	—	—	—	—

Dash means required power exceeds 2 MW, technically unfeasible in borehole conditions.

3.5. Frequency Dependence

Table 7. Relative efficiency at frequency detuning (line width 30 MHz, Lorentzian profile)

Δν [MHz]	0	5	10	15	20	25	30	40	50
g(Δν)/g(0)	1.00	0.96	0.85	0.69	0.53	0.39	0.28	0.14	0.07

3.7. Sensitivity Analysis

Table 8. Ranking of parameters by influence on productivity

Parameter	Elasticity	Uncertainty Range (orders of mag.)	Contribution to Uncertainty*
P_{diss}	1.0	10	10
n_{act}	1.0	6	6
σ	-1.2	3	3.6
P_{rad}	0.8	3	2.4
B_0	2.0	1	2
Line width	-0.3	0.6	0.18

*Contribution to Uncertainty = |Elasticity| × Uncertainty Range.

4. DISCUSSION

4.1. What Does the Conducted Modeling Provide?

1. **Quantitative Criteria:** For the first time, strict quantitative criteria have been obtained, delineating the regions of uselessness, laboratory interest, practical significance, and industrial application of the hypothetical resonant oxygen activation method.
2. **Focusing Experiments:** The modeling shows that experimental efforts should be directed towards determining two key parameters: the density of truly catalytically active Fe centers in Kuzbass coals (n_{act}) and the probability of water dissociation under the influence of an MHz-range field (P_{diss}). Without knowledge of these parameters, any discussion about the method's applicability remains speculative.
3. **Engineering Tool:** The nomogram (Fig. 2) and energy tables (Table 6) allow, for specific geological conditions (coal conductivity, Fe content) and technological constraints (available power, desired treatment radius), to assess whether the required P_{diss} value lies in a realistic region.
4. **Risk Identification:** The modeling confirms that the main practical risk is the accumulation of hydrogen to explosive concentrations. In the zone of practical significance (green zone in Table 2), the accumulation time is seconds to minutes, orders of magnitude less than diffusion removal time.

Consequently, any pilot or industrial installation must be equipped with a forced gas extraction system operating synchronously with the irradiation.

4.2. Model Limitations

1. **Phenomenological Nature of P_{diss}:** The model does not reveal the microscopic mechanism of water dissociation. The parameter P_{diss} was introduced phenomenologically and could depend on many factors (field strength, frequency, temperature, surface composition) not accounted for in this work.
2. **Idealized Kinetics:** The assumption $\theta_{H2O} \approx 1$ (all centers occupied by water) might be violated at high temperatures or in dry coals. Competition for centers from methane and other formation gas components was not considered.
3. **Homogeneity of Properties:** The model assumes a homogeneous distribution of properties (σ, n_{act}) within the treatment zone. Real coal seams are heterogeneous.
4. **Lack of Side Reactions:** Possible side reactions (formation of methanol, formaldehyde, oxidation of the coal itself) were not considered, which could affect the product balance and safety.

4.3. Comparison with Alternative Methods and Energy Efficiency

Table 9. Comparison of energy consumption for methane neutralization

Method	Energy Consumption, kWh/kg CH_4	Note
Thermal oxidation (combustion)	0.01–0.03	Heating gas only, excluding capital costs
Existing degassing methods	0.1–0.5	Drilling, vacuum, gas preparation [32]
Plasma-chemical oxidation	10–100	Laboratory data
Proposed method (this work)	**0.01–0.1**	Depending on R_{O2} and σ

Energy efficiency calculation for the proposed method:

For typical conditions (σ = 0.01 S/m, P_{rad} = 50 kW, treatment radius 20 m, zone volume V ≈ 25000 m³) and productivity at the practical significance threshold R_{O2} = 0.75 kg/(m³·h):

- Total oxygen generation: 0.75 kg/(m³·h) × 25000 m³ = 18750 kg O_2/h.
- This oxygen is sufficient for methane oxidation (via reaction $CH_4 + 2O_2 \rightarrow CO_2 + 2H_2O$): 18750 / 4 = 4688 kg CH_4/h.
- Specific energy consumption: 50 kW / 4688 kg/h ≈ 0.0107 kWh/kg CH_4.

If productivity increases to industrial levels (R_{O2} = 10 kg/(m³·h)), specific consumption drops to ~0.0008 kWh/kg CH_4. However, such values require correspondingly high dissociation probabilities $P_{diss} > 10^{-5}$ (see Table 2).

4.4. Program of Experimental Research (Refined)

Based on parametric modeling, the experimental research program should focus on determining n_{act} and P_{diss}:

Stage 1 (Laboratory, on Kuzbass coal samples):

1. Determine iron content and speciation (XPS, Mössbauer spectroscopy, EXAFS). Estimate the fraction of ultradispersed iron accessible on the pore surface.
2. Construct a laboratory setup with a 1.6 MHz generator, adjustable power (up to 1 kW), and a coil producing a field of 1–10 μT.
3. Place coal samples (natural moisture, controlled Fe content) in a sealed cell under a methane atmosphere.
4. Expose to the field for a set time (hours-days) with continuous mass spectrometric analysis of the gas phase (H_2, O_2, CO_2, CO, CH_4, possible organic products).
5. Conduct a series of experiments at varying frequencies, field strengths, moisture levels, and temperatures.

Stage 2 (Packed bed model): Tests on a scaled model to study transport processes and verify hydrogen safety criteria.

Stage 3 (Pilot): Field tests in a borehole only if Stage 1 and 2 results are positive, with a mandatory forced gas extraction system and continuous gas composition monitoring.

5. CONCLUSIONS

1. **Theoretical Foundations:** A calculation of a priori determinable parameters for the method of resonant oxygen activation in coal seams was performed. For Kuzbass conditions, the resonant frequency is 1.59–1.64 MHz. The penetration depth of the electromagnetic signal with a borehole

emitter is 40–130 m, depending on coal resistivity. The EPR line width of oxygen in coal (14–56 MHz) allows selecting a fixed frequency of 1.6 MHz for the entire basin.

2. **Key Uncertainties:** It is shown that direct electrolysis of water by macroscopic eddy currents is impossible. The possibility of water dissociation due to field concentration at micro-irregularities and resonant effects is the main uncertainty, introduced into the model as the phenomenological parameter P_{diss} (probability of dissociation per period). The second key parameter is the density of catalytically active Fe centers, n_{act} (estimated at 10^{14}–10^{16} m^{-2}).
3. **Parametric Modeling:** A complete mathematical model of the process was developed, combining electrodynamic, kinetic, and transport modules. Parameter scanning was performed across ranges: $n_{act} = 10^{12}$–10^{18} m^{-2}, $P_{diss} = 10^{-12}$–10^{-2}, $\sigma = 0.001$–1 S/m, $P_{rad} = 1$–1000 kW.
4. **Regime Maps and Nomograms:**
   - A phase diagram "site density – dissociation probability" was constructed, identifying regions of absolute uselessness, laboratory interest, practical significance, and industrial application. The boundary of practical significance (productivity 0.75 kg $O_2/(m^3 \cdot h)$) is described by the relation $n_{act} \cdot P_{diss} = 10^9$ m^{-2}.
   - Complete matrices for productivity and hydrogen accumulation time were generated for 64 combinations of key parameters, spanning 10 orders of magnitude.
   - An analytical dependence of the effective treatment radius on coal conductivity was derived: $r_{eff} \approx 20 \cdot (0.01/\sigma)^{0.4}$ m for $P_{rad} = 50$ kW. For typical Kuzbass coals ($\sigma \approx 0.01$ S/m), the radius is ~20 m, yielding a treatment zone volume of ~25000 m^3.
   - A nomogram was developed for engineering calculation of system parameter requirements based on geological conditions.
5. **Risk Analysis:** The main practical risk—hydrogen accumulation to explosive concentrations—was quantitatively confirmed. In the region of practical significance, accumulation time (seconds to minutes) is orders of magnitude less than diffusive removal time (hours to days). Therefore, any practical implementation of the method requires a mandatory forced gas extraction system operating synchronously with the irradiation.
6. **Energy Efficiency:** A correct calculation was performed considering the entire treated volume. At a productivity of 0.75 kg $O_2/(m^3 \cdot h)$ and power of 50 kW, specific energy consumption is ~0.01 kWh/kg CH_4. This is comparable to thermal oxidation and lower than the costs of existing degassing methods for inaccessible sorbed methane. This opens prospects for the method's economic viability upon successful experimental verification.
7. **Practical Recommendations:**
   - The method can be practically significant ONLY if all conditions are met: (a) $\sigma < 0.05$ S/m; (b) $n_{act} > 5 \cdot 10^{15}$ m^{-2}; (c) $P_{diss} > 2 \cdot 10^{-7}$; (d) $P_{rad} > 50$ kW; (e) presence of a gas extraction system.
   - The most promising for testing are high-resistivity coals (anthracites, lean coals) with a high content of ultradispersed iron.
   - Experimental efforts should be focused on determining n_{act} and P_{diss} under laboratory conditions on real Kuzbass coal samples.
8. **Conclusion:** The presented work does not prove the viability of the resonant oxygen activation method—this is fundamentally impossible without experiment. However, it creates a complete theoretical framework for its targeted experimental verification. The main outcome is parametric regime maps and nomograms that allow quantitatively determining the conditions under which the method could be practical and formulating requirements for system parameters. The obtained results serve as a basis for designing laboratory and pilot experiments.

ACKNOWLEDGMENTS

During the preparation of this work, the author used an AI language model for translation assistance from the original Russian manuscript and for language polishing. After using this tool, the author reviewed and edited the content as needed and takes full responsibility for the content of the publication.

Article prepared using parametric modeling and regime maps. Full text, 35 pages, 9 tables, 3 figures.

REFERENCES

[1] International Energy Agency. (2023). Global Methane Tracker 2023. IEA Publications. https://www.iea.org/reports/global-methane-tracker-2023

[2] Ruban, A.D., Zaburdyaev, V.S., & Zaburdyaev, G.S. (2020). Methane of coal seams: problems and solutions. Mining Informational and Analytical Bulletin, (5), 5-18. https://doi.org/10.25018/0236-1493-2020-5-0-5-18

[3] Kolesnichenko, I.E., Artemiev, V.B., & Kolesnichenko, E.A. (2018). Spontaneous combustion of coal: theory and practice. Moscow: Gornaya kniga.

[4] Voevodskiy, V.V., Molin, Yu.N., & Plyusnin, V.F. (2016). Electron paramagnetic resonance in chemistry. Novosibirsk: Publishing House of the Siberian Branch of the Russian Academy of Sciences.

[5] Terentiev, A.A., & Shenderovich, I.G. (1985). EPR of molecular oxygen in the gas phase and adsorbed state. Russian Chemical Reviews, 54(9), 1413-1440. https://doi.org/10.1070/RC1985v054n09ABEH003119

[6] Alken, P., Thébault, E., Beggan, C.D., et al. (2021). International Geomagnetic Reference Field: the thirteenth generation. Earth, Planets and Space, 73(1), 49. https://doi.org/10.1186/s40623-020-01288-x

[7] Landau, L.D., & Lifshitz, E.M. (2003). Electrodynamics of Continuous Media (4th ed.). Moscow: Fizmatlit.

[8] Landau, L.D., Lifshitz, E.M., & Pitaevskii, L.P. (1984). Electrodynamics of Continuous Media (2nd ed.). Oxford: Butterworth-Heinemann. (Course of Theoretical Physics, Vol. 8).

[9] Gurevich, A.M. (Ed.). (1983). Electrical properties of coals. Moscow: Nedra.

[10] Jackson, J.D. (1999). Classical Electrodynamics (3rd ed.). New York: Wiley.

[11] Gregg, S.J., & Sing, K.S.W. (1982). Adsorption, Surface Area and Porosity (2nd ed.). London: Academic Press.

[12] Panov, G.I., Dubkov, K.A., & Starokon, E.V. (2006). Active oxygen in selective oxidation catalysis. Catalysis Today, 117(1-3), 148-155. https://doi.org/10.1016/j.cattod.2006.05.014

[13] Dubkov, K.A., Ovanesyan, N.S., Shteinman, A.A., Starokon, E.V., & Panov, G.I. (2002). Kinetics of the redox reaction of FeZSM-5 with CO and N2O. Journal of Catalysis, 207(2), 341-352. https://doi.org/10.1006/jcat.2002.3552

[14] Starokon, E.V., Parfenov, M.V., Pirutko, L.V., Abornev, S.I., & Panov, G.I. (2011). Oxidation of methane to methanol on the surface of FeZSM-5. Journal of Catalysis, 281(1), 54-61. https://doi.org/10.1016/j.jcat.2011.04.002

[15] Huggins, F.E., & Huffman, G.P. (1987). Mössbauer analysis of iron-bearing phases in coal, coke, and ash. In G.J. Long & J.G. Stevens (Eds.), Mössbauer Spectroscopy Applied to Inorganic Chemistry (Vol. 2, pp. 417-444). New York: Plenum Press.

[16] Huggins, F.E., & Huffman, G.P. (1991). Mössbauer analysis of iron-bearing phases in coal and coal ash. In S.N. Mukherjee (Ed.), Chemistry of Coal and Coal Products. Advances in

Chemistry Series, Vol. 248 (pp. 123-136). Washington, DC: American Chemical Society. https://doi.org/10.1021/ba-1991-0248.ch007

[17] Lefevre, M., Proietti, E., Jaouen, F., & Dodelet, J.P. (2009). Iron-based catalysts with improved oxygen reduction activity in polymer electrolyte fuel cells. Science, 324(5923), 71-74. https://doi.org/10.1126/science.1170051

[18] Rimstidt, J.D., & Vaughan, D.J. (2003). Pyrite oxidation: a state-of-the-art assessment of the reaction mechanism. Geochimica et Cosmochimica Acta, 67(5), 873-880. https://doi.org/10.1016/S0016-7037(02)01165-1

[19] Weil, J.A., & Bolton, J.R. (2007). Electron Paramagnetic Resonance: Elementary Theory and Practical Applications (2nd ed.). Hoboken: Wiley-Interscience.

[20] Galkina, O.G., Lunina, E.V., & Mashkovskiy, D.A. (1998). EPR of oxygen adsorbed on carbon materials. Russian Journal of Physical Chemistry, 72(5), 912-916.

[21] Nikitin, A.P., Valnyukova, A.S., Furega, R.I., Cherkasova, T.G., & Patrakov, Yu.F. (2018). Development of a method for recording EPR spectra of coals. Vestnik of Kuzbass State Technical University, (5), 76-82. https://doi.org/10.26730/1999-4125-2018-5-76-82

[22] Nikitin, A.P., Valnyukova, A.S., Cherkasova, T.G., Patrakov, Yu.F., & Furega, R.I. (2021). Study of fossil coals in the Kuznetsk basin by EPR spectroscopy. Journal of Physics: Conference Series, 1749, 012018. https://doi.org/10.1088/1742-6596/1749/1/012018

[23] Dzhadan, M., Nur, H.A., Adashkevich, S.V., Stelmakh, V.F., et al. (2008). Calibration samples based on carbon for EPR spectroscopy. In Materials and structures of modern electronics: Proceedings (pp. 92-96). Minsk: BSU.

[24] Kuznetsk coal basin. (2017). In Great Russian Encyclopedia. Moscow. https://bigenc.ru/geography/text/5279432

[25] Ammosov, I.I., & Eremin, I.V. (Eds.). (1969). Geology of coal basins and deposits of the USSR. Vol. 7: Kuznetsk basin. Moscow: Nedra.

[26] Kuzbassrazrezugol digitizes sections of coal mines. (2023, November 21). Kontinent Sibir Online. https://ksonline.ru/516521/kuzbassrazrezugol-otsifrovyvaet-uchastki-ugolnyh-razrezov/

[27] Ministry of Digital Development and Communications of Kuzbass. Geographic Information System "Kuzbass". https://digital42.ru/deyatelnost/gis-kuzbass/

[28] Stepanov, Yu.A., & Burmin, L.N. (2024). Method for constructing a digital twin of a coal-rock mass for modeling the integrated development of the Kuzbass subsurface. Geoinformatika, (1), 57-65. https://doi.org/10.47148/1609-364X-2024-1-57-65

[29] Rosgeolfond. Service for access to electronic information. https://reports.geologyscience.ru/

[30] Vilker, V.G., & Pavlenko, M.V. (1998). On parameters of vibrational impact on coal massif to increase methane yield of coal. Mining Informational and Analytical Bulletin, (3), 45-49.

[31] Fujishima, A., Zhang, X., & Tryk, D.A. (2008). TiO2 photocatalysis and related surface phenomena. Surface Science Reports, 63(12), 515-582. https://doi.org/10.1016/j.surfrep.2008.10.001

[32] Zaburdyaev, V.S. (2015). Energy consumption during degassing of coal mines. Ugol, (8), 12-16. https://doi.org/10.18796/0041-5790-2015-8-12-16

[33] Sang, G., Liu, S., Zhang, R., Elsworth, D., & He, L. (2020). Hydrogen storage in coal: a review. International Journal of Hydrogen Energy, 45(55), 28745-28760. https://doi.org/10.1016/j.ijhydene.2020.07.252

[34] Thauer, R.K., Kaster, A.K., Seedorf, H., Buckel, W., & Hedderich, R. (2008). Methanogenic archaea: ecologically relevant differences in energy conservation. Nature Reviews Microbiology, 6(8), 579-591. https://doi.org/10.1038/nrmicro1931

[35] Kohen, A., & Klinman, J.P. (1999). Hydrogen tunneling in biology. Chemistry & Biology, 6(7), R191-R198. https://doi.org/10.1016/S1074-5521(99)80058-1